DOI 10.5012/bkcs.2009.30.12.2973

Ab Initio Study on the Thermal Decomposition of CH_3CF_2O Radical

Hari Ji Singh,* Bhupesh Kumar Mishra, and Nand Kishor Gour

Department of Chemistry, DDU Gorakhpur University, Gorakhpur-273009, U. P. India
**E-mail: hari_singh81@hotmail.com*
Received July 31, 2009, Accepted October 14, 2009

The decomposition reaction mechanism of CH_3CF_2O radical formed from hydroflurocarbon, CH_3CHF_2 (HFC-152a) in the atmosphere has been investigated using *ab-initio* quantum mechanical methods. The geometries of the reactant, products and transition states involved in the decomposition pathways have been optimized and characterized at DFT-B3LYP and MP2 levels of theories using 6-311++G(d,p) basis set. Calculations have been carried out to observe the effect of basis sets on the optimized geometries of species involved. Single point energy calculations have been performed at QCISD(T) and CCSD(T) level of theories. Out of the two prominent decomposition channels considered viz., C-C bond scission and F-elimination, C-C bond scission is found to be the dominant path involving a barrier height of 12.3 kcal/mol whereas the F-elimination path involves that of a 28.0 kcal/mol. Using transition-state theory, rate constant for the most dominant decomposition pathway viz., C-C bond scission is calculated at 298 K and found to be 1.3×10^4 s^{-1}. Transition states are searched on the potential energy surfaces involving both decomposition channels and each of the transition states are characterized. The existence of transition states on the corresponding potential energy surface are ascertained by performing Intrinsic Reaction Coordinate (IRC) calculation.

Key Words: HFC-152a, Decomposition of HFC, PES. Transition state theory

Introduction

It is now well established that atomic chlorine transported to the stratosphere by release of a variety of chlorine containing compounds particularly chlorofluorocarbons (CFCs) is responsible for the depletion of ozone layer in this region of atmosphere. CFCs give rise to perhaps the most well known and disastrous environmental problem of destruction of stratospheric ozone layer.[1-4] CFCs were developed in late 1920s in the search for more friendly refrigerants as substitutes for ammonia and sulphur-dioxide. The chemical inertness of CFCs which is one of the desired properties is also the properties that cause them to be environmentally unfriendly. Once released in the atmosphere CFCs remains there for a longer period of time because they do not react with OH or NO_2 radicals formed in the atmosphere. However, it absorbs short wavelengths UV radiations generating Cl free radicals responsible for the catalytic destruction of ozone layer. The threat of CFCs to the ozone layer was considered so serious that an international treaty (1987 Montréal Protocol) was developed to prohibit production and use of CFCs and most other chemicals causing ozone depletion.

After the global alarm about the deleterious effect of CFCs in the atmosphere, serious efforts for finding out substitutes of these stable CFCs are made during the past decades. Various hydrofluorocarbons (HFCs) and hydrochloroflurocarbons (HCFCs) having physicochemical properties similar to CFCs have been synthesized and put into global use as an alternative to CFCs.[5-6] The essential advantages shared by the proposed substitutes with respect to their ozone depletion potential are their incomplete halogenation. HFCs have been proposed as environmentally friendly replacement for CFCs in many applications primarily because the former have little potential for contributing to stratospheric ozone destruction as HFCs contain no chlorine to catalyze stratospheric ozone.[7] On the other hand they do contain alkyl hydrogen which is readily abstracted by atmospheric hydroxyl radicals, initiating its tropospheric decomposition.[8]

One of the most widely used HFC as an alternative to trichlorofluoromethane (CFC-11) and dichlorofluoromethane (CFC-12) is 1,1-difluoroethane (HFC-152a). HFC-152a is a colorless flammable gas with a slight ethereal odor used as a non-ozone depleting aerosol propellant and as an alternative in foam applications. Other potential uses include refrigeration blends and catalyst regeneration. Its global warming potential (GWP) is determined to be 140 relative to CO_2[9] due to its relatively short tropospheric lifetime of about one and a-half year. HFC-152a is degraded into the atmosphere by reaction with photochemically produced hydroxyl radicals.[10] This is the dominant path for removing these compounds from troposphere. A general mechanism of tropospheric degradation mechanism of HFC-152a may be shown as follows:

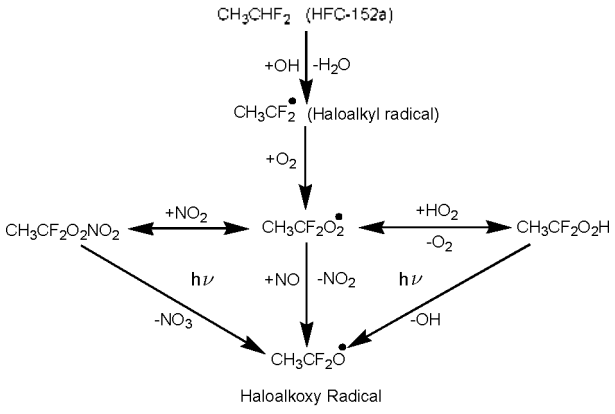

Scheme 1. Tropospheric degradation mechanism of HFC-152a

The above scheme is based on the fact that the initial attack of OH radical on HFC-152a leads to the formation of haloalkyl radical ($CH_3CF_2^{\bullet}$) which in turn react with atmospheric O_2 to give peroxy radicals ($CH_3CF_2O_2^{\bullet}$).[11] The latter react further with NO leading to the formation of haloalkoxy radical ($CH_3CF_2O^{\bullet}$) *via* a short-lived intermediate, the peroxynitrate ($CH_3CF_2O_2NO_2$). On the other hand haloalkoxy radical may also be generated through another intermediate, the hydroperoxide ($CH_3CF_2O_2H$) formed by the reaction of $CH_3CF_2O_2$ and HO_2 radicals. The haloalkoxy radicals thus formed play an important role in the degradation mechanism of organic compounds in the troposphere.[12-13] There are two potentially accessible decomposition pathways that involve C-C bond scission and F-elimination as shown below:

$$CH_3CF_2O \longrightarrow CH_3 + CF_2O \quad (1)$$

$$\longrightarrow CH_3C(O)F + F \quad (2)$$

Studying the fate of haloalkoxy radicals thus formed is important from the viewpoint of understanding its role in atmospheric chemistry. A few experimental study of the decomposition of $CH_3CF_2O^{\bullet}$ radical was carried out by Wallington *et al.*[14] No theoretical evidence is reported to date. To explain the experimental results and to predict the new characteristics about the loss of $CH_3CF_2O^{\bullet}$ radical, a theoretical investigation is most desirable. In this paper we present a theoretical study on the thermal decomposition of $CH_3CF_2O^{\bullet}$ radical using the high-level *ab-initio* molecular orbital method.

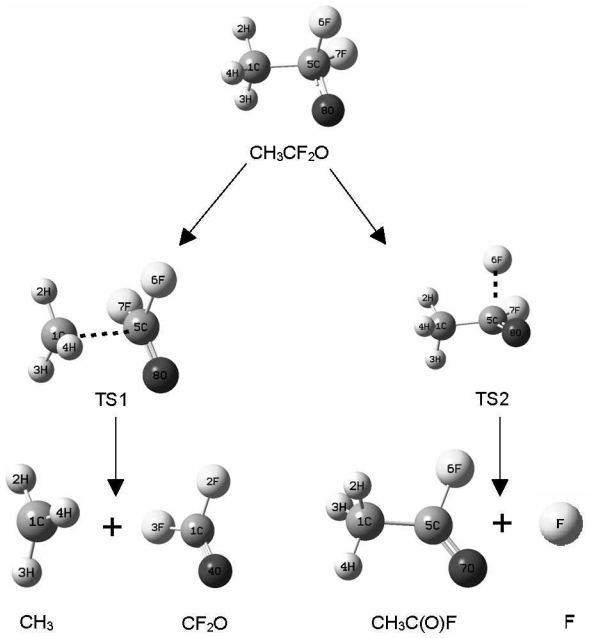

Figure 1. Optimized geometries of reactant, products and transition states involved in the decomposition of CH_3CF_2O using B3LYP/6-311++G(d,p) method.

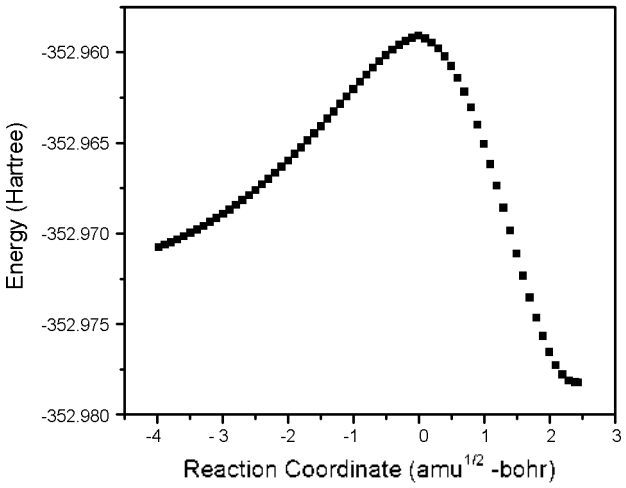

Figure 2. IRC plot for the transition state TS1 for C-C bond scission in the CH_3CF_2O decomposition.

Computational Method

Ab-initio quantum mechanical calculations[15] were performed with the GAUSSIAN03[16] package. Geometry optimization of the reactant, products and transition states were performed using density functional study (DFT) employing Becke's three-parameter hybrid functional (B3LYP)[17-18] with the 6-311++G(d,p) basis set. The vibrational frequencies were obtained at the same level to determine the nature of different stationary points on the potential energy surface. All the stationary points have been identified to be the minima with no imaginary frequency (NIMAG = 0) and the transition states with one imaginary frequency (NIMAG = 1). To ascertain that the identified transition states connect reactant and products smoothly, Intrinsic Reaction Coordinate (IRC) calculations[19-20] were performed at the B3LYP/6-311++G(d,p) level. In order to refine the energy values, single-point energy calculations were performed at the QCISD(T)[21] and CCSD(T)[22] level of theories using fairly large basis sets such as 6-311++G(3df,3pd). In order to correct the total energy, zero-point energy calculations were made at B3LYP/6-311++G(d,p) level.[17,18]

Results and Discussion

The fate of haloalkoxy radical (CH_3CF_2O) considered during the course of present investigation is predominantly its thermal decomposition in the atmosphere. Two dominant decomposition pathways considered (reactions 1 and 2) involve transition states TS1 and TS2 respectively. Optimized geometries of reactant, products and transition states were done at B3LYP/6-311++G(d,p) and MP2/6-311++G(d,p) level of theories. Results obtained at B3LYP level are shown in Figure 1. Geometrical parameters obtained at both levels are recorded in Table 1. The results show that structural parameters are almost the same with both methods except in the case of TS1 structure. In the optimized structure of TS1 the elongation of the C-C bond using B3LYP method is found to be 2.046 Å whereas at MP2 the value is only 1.870 Å. Results obtained during frequency calculations for reactant, products and transition

Table 1. Structural parameters of reactant, products and transition states involved in CH_3CF_2O decomposition at B3LYP/6-311++G(d,p) (first line) and MP2/6-311++G(d,p) (second line)

	CH_3CF_2O	TS1	TS2	CH_3	CF_2O	$CH_3C(O)F$
Bond length (Å)						
R (C1-C5)	1.536	2.046	1.491	-	-	1.495
	1.513	1.870	1.493	-	-	1.495
R (C5-O8)	1.326	1.200	1.225	-	-	-
	1.347	1.200	1.220	-	-	-
R (C5-O7)	-	-	-	-	-	1.182
	-	-	-	-	-	1.188
R (C1-O4)	-	-	-	-	1.171	-
	-	-	-	-	1.176	-
R (C1-H2)	1.093	1.084	1.094	1.081	-	1.092
	1.090	1.086	1.093	1.079	-	1.092
R (C1-H3)	1.088	1.082	1.089	1.081	-	1.092
	1.089	1.08	1.089	1.079	-	1.092
R (C1-H4)	1.088	1.082	1.087	1.081	-	1.087
	1.089	1.083	1.087	-	-	1.087
R (C5-F6)	1.375	1.355	1.952	-	-	1.373
	1.362	1.353	1.796	-	-	1.367
R (C5-F7)	1.375	1.355	1.342	-	-	-
	1.362	1.353	1.335	-	-	-
R (C1-F2)	-	-	-	-	1.322	-
	-	-	-	-	1.318	-
R (C1-F3)	-	-	-	-	1.322	-
	-	-	-	-	1.318	-
Bond Angle (deg)						
A (H2-C1-H3)	110.057	117.282	108.436	119.984	-	107.422
	109.777	116.316	109.072	119.999	-	107.713
A (H2-C1-H4)	110.057	117.282	110.039	120.001	-	110.260
	110.500	116.316	111.375	120.00	-	110.260
A (H3-C1-H4)	110.804	116.965	109.624	120.016	-	110.256
	110.500	116.609	109.969	120.002	-	110.438
A (C1-C5-F6)	110.318	97.803	102.516	-	-	110.263
	110.964	100.054	111.686	-	-	109.950
A (F6-C5-F7)	105.042	106.382	99.729	-	-	-
	105.481	105.714	100.753	-	-	-
A (F6-C5-O8)	111.982	123.139	81.924	-	-	-
	110.598	122.819	82.288	-	-	-
A (F6-C5-O7)	-	-	-	-	-	119.874
	-	-	-	-	-	120.304
A (F2-C1-F3)	-	-	-	-	108.289	-
	-	-	-	-	107.484	-
A (F2-C1-O4)	-	-	-	-	125.856	-
	-	-	-	-	126.257	-

states using both methods are recorded in Table 2. The result shows that value obtained using MP2 method are slightly higher than that of B3LYP. These results also show that the reactant and products have stable minima on their potential energy surface characterized by the occurrence of real vibrational frequencies. Transition states TS1 and TS2 are characterized by the occurrence of only one imaginary frequency as obtained during the frequency calculation. Results recorded in Table 2 show the values at 453 and 285 cm^{-1} for TS1 and TS2 respectively at B3LYP level whereas at MP2 the respective values are 768 and 1163 cm^{-1}. These frequencies are analyzed using the GaussView program.[23] Visualization of vibrations corresponding to the calculated imaginary frequencies show the well defined transition state geometries connecting reactant and products during transition. In order to ascertain the existence of transition state on the potential energy surface Instrinsic Reaction Coordinate (IRC) calculations are also performed for each of the transition states determined. The IRC plots for TS1 and TS2 are shown in Figs 2 and 3 respectively. The IRC calculations show that each transition state smoothly connects the reactant and products on the potential energy surface. Visualization of the optimized structure of TS1 reveals the elongation of C-C bond length (1.536 Å to 2.046 Å at B3LYP and 1.513 Å to 1.870 Å) with a simultaneous shrinkage of the C-O distance from 1.326 Å to 1.20 Å and forming a carbon-oxygen double bond. Similarly the structure of TS2 reveals the elongation of C-F bond length from 1.375 Å to 1.952 Å at B3LYP and 1.362 Å to 1.796 Å at MP2 accompanied by a

Table 2. Unscaled vibrational frequencies of reactant, products and transition states in CH_3CF_2O decomposition at B3LYP/6-311++G(d,p) (first line) and MP2/6 311++G(d,p) (second line) levels of theory

Species	Vibrational frequencies (cm^{-1})
CH_3CF_2O	173, 327, 349, 524, 530, 537, 790, 896, 922, 1059, 1149, 1233, 1385, 1445, 1485, 3052, 3141, 3170 214, 339, 363, 526, 551, 563, 840, 941, 972, 1202, 1209, 1287, 1421, 1489, 1506, 3116, 3220, 3233
TS1	**453i**, 128, 230, 250, 533, 563, 567, 649, 661, 859, 1062, 1081, 1414, 1427, 1682, 3090, 3255, 3264 **768i**, 184, 284, 316, 553, 590, 614, 791, 800, 892, 1111, 1165, 1443, 1463, 1694, 3139, 3309, 3332
TS2	**285i**, 159, 171, 271, 422, 487, 587, 840, 1007, 1027, 1222, 1402, 1458, 1471, 1613, 3050, 3125, 31 **1163i**, 201, 241, 316, 441, 527, 606, 872, 997, 1047, 1256, 1419, 1483, 1494, 1624, 3109, 3206, 32
$CH_3C(O)F$	124, 414, 570, 596, 816, 1000, 1068, 1180, 1403, 1469, 1474, 1912, 3051, 3112, 3159 133, 420, 573, 601, 836, 1020, 1076, 1206, 1421, 1489, 1495, 1902, 3110, 3197, 3235
CH_3	537, 1401, 1403,3102,3281,3283 462, 1445, 1446, 3176, 3370, 3371
CF_2O	575, 614, 772, 955, 1201, 1974 586, 620, 783, 965, 1232, 1974

Table 3. Zero-point energy corrected total energies for species involved in C-C bond scission from CH_3CF_2O decomposition. [Geometries were optimized at B3LYP/6-311++G (d,p) level] (unit: hartree)

Method	CH_3CF_2O	TS1	CH_3	CF_2O
CCSD(T)/6-311+G(d)	-352.133911	-352.111880	-39.677750	-312.448031
CCSD(T)/6-311+G(d,p)	-352.156806	-352.135128	-39.705041	-312.450499
CCSD(T)/6-311++G(d,p)	-352.157072	-352.135432	-39.705194	-312.450499
CCSD(T)/6-311G(d,p)	-352.139472	-352.118554	-39.703765	-312.436842
CCSD(T)/6-311++G(3df,3pd)	-352.363068	-352.343380	-39.729701	-312.627872
QCISD(T)/6-311+G(d,p)	-352.158037	-352.137219	-39.705094	-312.449439
QCISD(T)/6-311G(d,p)	-352.140512	-352.120484	-39.700871	-312.435955
ZPE B3LYP/6-311++G(d,p)	0.050517	0.047205	0.029651	0.013875

shrinkage of the C-O bond as recorded in Table 1.

Single point energy calculations of various species involved in the decomposition pathways are performed using CCSD (T) and QCISD(T) level of theories at B3LYP/6-31++G(d.p) optimized geometries. In order to refine the values, these calculations are also performed using larger basis sets incorporating polarized and diffused basis sets. Calculated total energies are corrected for zero-point energy, the latter being calculated at B3LYP using 6-311++G(d,p) basis using a scale factor of 0.96.[15] Zero-point corrected total energies using standard and extended basis sets for various species and transition states involved in decomposition reactions (1) and (2) are recorded in Tables 3 and 4. The computed data shows that most favorable decomposition channel for CH_3CF_2O is the C-C bond scission involving an energy barrier of 12.3 kcal mol^{-1}. The associated energy barriers corresponding to decomposition pathways of CH_3CF_2O calculated from the results obtained at various level of theories are shown in Table 5. These results show that energy barrier for C-C bond scission is in the range of 12 - 13 kcal/molwhereas for F-elimination it is in the range of 26 - 28 kcal/mol depending upon the levels of theories involved during the calculation. Literature survey reveals that there is no experimental data available for the comparison of these energy barriers for the corresponding decomposition pathways of CH_3CF_2O radical. However, to ascertain the reliability of the calculated values during the course of the present

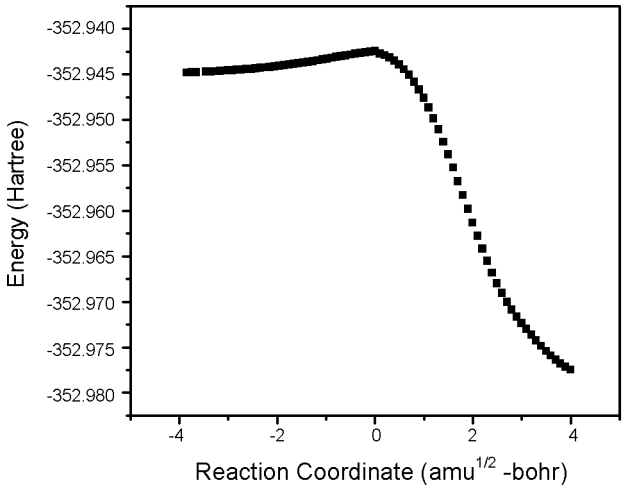

Figure 3. IRC plot for the transition state TS2 for F-elimination in the CH_3CF_2O decomposition.

Table 4. Zero-point energy corrected total energies for species involved in F-elimination from CH_3CF_2O decomposition. [Geometries optimized at B3LYP/6

Method	CH_3CF_2O	TS2	$CH_3C(O)F$	F
CCSD(T)/6-311+G(d)	-352.133911	-352.091590	-252.528892	-99.571581
CCSD(T)/6-311+G(d,p)	-352.156806	-352.114237	-252.551730	-99.571581
CCSD(T)/6-311++G(d,p)	-352.157072	-352.114488	-252.551928	-99.571581
CCSD(T)/6-311G(d,p)	-352.139472	-352.095662	-252.540308	-99.565746
CCSD(T)/6-311++G (3df,3pd)	-352.363068	-352.318447	-252.704410	-99. 61769
QCISD(T)/6-311+G(d,p)	-352.158037	-352.116335	-252.552955	-99.571685
QCISD(T)/6-311G(d,p)	-352.140512	-352.097519	-252.541440	-99.565804
ZPE B3LYP/6-311++G(d,p)	0.050517	0.048959	0.048649	0.000

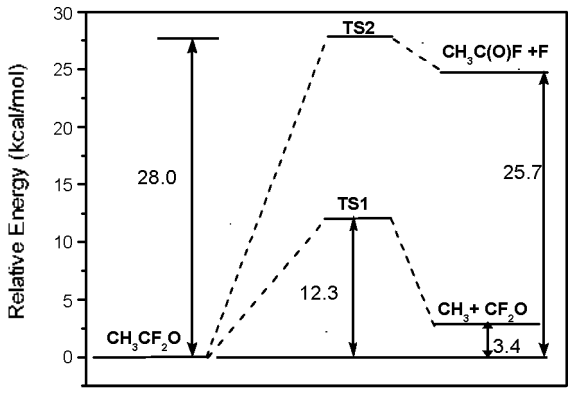

Figure 4. Energy diagram for CH_3CF_2O decomposition channels calculated at CCSD(T)/6-311++G(3df,3pd) level on the geometries optimized at B3LYP/6-311++G(d,p) level.

study using a particular method a comparison is made with the energy values calculated by Hou *et al.*[24] for a structurally similar compound CH_3CHFO made at a considerably higher level using G2//MP2/6-31G(d) method. In CH_3CHFO the energy barrier for C-C bond scission has been shown to be 11.6 kcal/mol[24] whereas the calculated value during the present study for C-C bond scission in CH_3CF_2O is 12.3 kcal/mol at CCSD (T) level with the largest basis set used. These values show a good agreement. This gives us a confidence to use single point energy calculation data obtained using CCSD(T)/6-311++G (3df.3pd) method on the geometries optimized at B3LYP/6-311++G(d,p) level to calculate energy barriers for two decomposition channels of CH_3CF_2O radical considered in the present study. An energy diagram is constructed (Figure 4) with the zero-point corrected energies data recorded in Tables 4 and 5 relative to the ground state energy of CH_3CF_2O arbitrarily taken as zero. The barrier height of 12.3 kcal mol^{-1} for C-C bond scission is considerably lower than that corresponding to F-elimination process. This makes the C-C bond scission pathway as the dominant process for the dissociation of this haloalkoxy radical in the atmosphere. Results recorded in Table 5 also show that energy barriers calculated using polarized function is slightly higher than that without polarized functions. Spin contamination is not important for the CH_3CF_2O radical because $<S^2>$ is in the range of 0.758 at HF/6-31G(d) to 0.76 at MP2/6-311++G(d,p) before annihilation that are only slightly larger than the expected value of $<S^2> = 0.75$ for doublets.

Table 5. Calculated energy barriers in kcal mol^{-1}

Method	C-C bond scission	F-elimination
CCSD(T)/6-311G(d,p)	13.1	26.5
CCSD(T)/6-311+G(d,p)	13.6	26.7
QCISD(T)/6-311G(d,p)	12.6	26.9
QCISD(T)/6-311+G(d,p)	13.0	26.1
CCSD(T)/6-311++G(3df,3pd)	12.3	28.0

Rate Constants

The rate constants of decomposition reactions (1) and (2) of CH_3CF_2O radical is calculated using Canonical Transition State Theory (CTST)[25] that involves a semi-classical one-dimensional multiplicative tunneling correction factor. The rate constants are computated using the following expression:

$$k = \Gamma(T)\frac{k_B T}{h}\frac{Q^{\ddagger}_{TS}}{Q_R} exp\frac{-\Delta E}{RT} \quad (3)$$

where $\Gamma(T)$ is the tunneling correction factor at temperature T. $Q^{\ddagger}_{TS}$ and Q_R are the total partition functions for the transition state and reactant respectively. ΔE. k_B and h are the barrier height. Boltzmann's and Planck's constants respectively. We adopted the simple and computationally inexpensive Wigner's method[26] for the estimation of the tunneling correction factor using the expression

$$\Gamma(T) = 1 + \frac{1}{24}\left|\frac{h\nu^{\ddagger}}{k_B T}\right|^2 \quad (4)$$

where $\nu^{\ddagger}$ is the imaginary frequency at the saddle point. The tunneling correction factor $\Gamma(T)$ is found to be almost unity. The partition functions for the respective transition state and reactant at 298 K are obtained from the harmonic vibrational frequencies calculated at the B3LYP/6-311++G(d,p) level. The rate constant for C-C bond scission in CH_3CF_2O decomposition is calculated to be 1.3×10^4 s^{-1} at 298 K and 1 atm pressure. Literature survey reveals that there is no experimental available in the literature to make a comparison with the calculated values obtained during the present investigation. However, based on an analogy with the decomposition of other oxy-radicals for C-C bond scission, our calculated value comes

out to be of the same order of magnitude.[27] Our modeling calculation also results the A-factor for C-C bond scission to be 1.3×10^{13} s^{-1} which is also in good agreement with the value of 1.1×10^{13} s^{-1} for CH_3CH_2O obtained by Caralp *et al.*[28] Similarly, the rate constant for F-elimination *via* reaction 2 involving TS2 as the transition state is calculated to be 4.4×10^{-8} s^{-1} at 298 K and 1 atm pressure with the associated A factor of 1.4×10^{13} s^{-1}.

Conclusion

The most important stationary points on the potential energy surface for the thermal decomposition of CH_3CF_2O radical are investigated using *ab-initio* quantum mechanical methods QCISD(T) and CCSD(T) of the geometries optimized at B3LYP/6-311++G(d,p) for all the species involved during the decomposition channels of CH_3CF_2O radical. Energetic calculation reveals that the most dominant decomposition pathways for CH_3CF_2O is the C-C bond scission using a barrier height of 12.3 kcal mol^{-1} in comparison to the F elimination process occurring with a barrier height of 28.0 kcal mol^{-1}. The thermal rate constant evaluated using conventional transition state theory for the C-C bond scission decomposition pathway is found to be 1.3×10^{4} s^{-1} at 298 K and 1 atm pressure.

Acknowledgments. The authors are thankful to University Grants Commission, New Delhi for providing fellowships to BKM and NKG under its DSA (Phase-I) program to the Department of Chemistry, DDU Gorakhpur University, Gorakhpur.

References

1. Molina, M. J.; Rowland, F. S. *Nature* **1974**, *249*, 810.
2. Anderson, J. G.; Toohey, D. W.; Brune, W. H. *Science* **1991**, *39*, 251.
3. Rowland, F. S. *Ambio.* **1990**, *19*, 281.
4. Rowland, F. S.; Molina, M. J. *Chem. Eng. News.* **1994**, *8*, 72.
5. Hoffman, J. S. *Ambio.* **1990**, *19*, 329.
6. Solomon, S. *Nature* **1990**, *347*, 6291.
7. Rowland, F. S. *Ann. Rev. Phys. Chem.* **1991**, *42*, 731.
8. Atkinson, R. In Scientific Assessment of Stratospheric Ozone, Vol II. World Meteorological Organization Global Ozone Research and Monitoring Project report No-20, 1989.
9. World Meteorological Organization. Scientific Assessment of Ozone Depletion Report No 47, Global Ozone Research and Monitoring Project, 2002.
10. Gierczak, T.; Talukdar, R.; Vaghjiani, G. L.; Lovejoy, E. R.; Ravishankara, A. R. *J. Geophys. Rev.* **1991**, *96*, 5001.
11. Atkinson, R. *J. Phys. Chem.* **1989**, *18*, 1.
12. Brasseur, G. P.; Orlando, J. J. *Atmospheric Chemistry and Global Change*; Oxford University Press: New York, 1999.
13. Wallington, T. J.; Hurley, M. D. Francheboud, J. M.; Orlando, J. J.; Tyndall, G. S.; Sehested, J.; Mogelberg,T. E.; Nielsen, O. J. *J. Phys. Chem.* **1996**, *100*, 18116.
14. Wallington, T. J.; Hurley, M. D.; Anderson, M. P.; Toft, A. *J. Phys. Chem A* **2005**, *109*, 9061.
15. Hehre, W. J.; Radom, L.; Schleyer, P. V. R.; Pople, J. A. *Ab Initio Molecular Orbital Theory*; Wiley: New York. 1986.
16. Frisch, M. J. *et al.* Gaussian 03 (Revision C.02); Gaussian Inc.; Wallingford, CT, 2004.
17. Becke, A. D. *J. Chem. Phys.* **1993**, *98*, 5648.
18. Lee, C.; Yang, W.; Parr, R. G. *Phys. Rev.* **1988**, *37*, 785.
19. Gonzalez, C.; Schlegel, H. B. *J. Chem. Phys.* **1989**, *90*, 2154.
20. Gonzalez, C.; Schlege, H. B. *J. Chem. Phys.* **1990**, *94*, 5523.
21. Pople, J. A.; Head-Gordan, M.; Raghavachari, K. *J. Chem, Phys.* **1987**, *87*, 5968.
22. Watts, J. D.; Gauss, J.; Bartlett, R. J. *Chem. Phys. Lett.* **1992**, *200*, 1.
23. Frisch, A.; Nielsen, A. B.; Holder, A. J. *GaussView Users Manual*; Gaussian Inc.: 2000.
24. Hou, H.; Wang, B. *Phys. Chem. Chem. Phys.* **2000**, *2*, 61.
25. Truhlar, D. G.; Garrett, B. C.; Klippenstein, S. J. *J. Phys. Chem.* **1996**, *100*, 12771.
26. Wigner, E. P. Z. *Phys. Chem.* **1932**, *B19*, 203.
27. Stevens, J. E.; Khayat, R. A. J.; Radkevich, O.; Brown, J. *J. Phys. Chem.* **2004**, *108*, 11354.
28. Caralp, F.; Devolder, P.; Fittschen, C.; Gomez, N.; Hippler, H.; Mereau, R.; Rayez, M. T.; Striebel, F.; Viskolcz, B. *Phys. Chem. Chem. Phys.* **1999**, *1*, 2935.